Indian Journal of Chemistry
Vol. 65, April 2026, pp. 316-327
DOI: 10.56042/ijc.v65i4.20939

Synthesis and multitarget activity of thiadiazole–thiocoumarin hybrids: A new class of broad-spectrum anti-infective agents

Navin B Patel[a], Monika R Tiwari[a], Ankita S Gamit[b], Tejal R Humal[c], Rogelio Gomez-Escobedo[d], Benjamín Nogueda-Torres[d], Gildardo Rivera[e] & Vatsal M Patel*[c]

[a] Department of Chemistry, Veer Narmad South Gujarat University, Udhana-Magdalla Road, Surat 395 007, Gujarat, India

[b] Department of Chemistry, Shri J. S. Bhakta and Shri K. M. Bhakta Arts Shri A. N. Shah Science and Shri N. F. Shah Commerce College, Kholwad, Surat 394 185, Gujarat, India

[c] Department of Chemistry, Jamanaben Narottambhai Motiram Patel Science College, Bharthana (Vesu), Surat 395 017, Gujarat, India

[d] Departamento de Parasitología, Escuela Nacional de Ciencias Biológicas, Instituto Politécnico Nacional, Ciudad de México 07738, Mexico

[e] Laboratorio de Biotecnología Farmacéutica, Centro de Biotecnología Genómica, Instituto Politécnico Nacional, Reynosa 88710, Mexico

E-mail: patelvatsal1904@gmail.com

Received 24 June 2025; accepted (revised) 9 April 2026

Emerging resistance across infectious pathogens has escalated the demand for chemotherapeutics with multitarget efficacy and minimal cytotoxicity. Herein, we report synthesizing a novel series of thiadiazole–thiocoumarin hybrid derivatives (A1–A10), designed to integrate redox activity with pharmacophoric rigidity. These compounds have been evaluated for a spectrum of biological activities, including trypanocidal, antitubercular, antimalarial, antimicrobial, and antioxidant potential. The synthesized hybrids display varying degrees of efficacy against *Trypanosoma cruzi* (NINOA and INC-5 strains), *Mycobacterium tuberculosis* H37Rv, *Plasmodium falciparum*, and multiple bacterial and fungal strains. Among the series, compound A9 shows exceptional trypanocidal and antitubercular activity (LC_{50} = 35.69 µM; MIC = 62.5 µg/mL), while A6 exhibits potent antimalarial effects (IC_{50} = 0.58 µg/mL), and A10 demonstrates the highest antibacterial activity. The antioxidant profile reveals A8 and A2 as strong radical scavengers *via* DPPH and ABTS assays. Structure-activity relationship (SAR) analysis indicates that electron-withdrawing groups favour trypanocidal activity but often increased cytotoxicity, whereas electron-donating or moderately lipophilic substituents improve selectivity. Notably, most compounds exhibit low toxicity in J774A macrophages, yielding favorable selectivity indices. Collectively, these findings highlight thiadiazole-thiocoumarin hybrids as versatile scaffolds for developing next-generation antiparasitic and antimicrobial agents.

Keywords: Thiadiazole, Thiocoumarin, Trypanocidal, Antitubercular, Antimalarial, Antioxidant, Structure-Activity Relationship, Multitarget Agents

In recent years, heterocyclic compounds with five-membered rings containing sulfur, oxygen, and nitrogen have exhibited remarkable chemical behavior and a wide range of versatile biological activities. The bioactive molecules containing the thiadiazol ring have been increasingly identified and investigated[1-4]. Thiadiazole contains two nitrogen atoms and one sulfur atom in its ring structure[5]. Thiadiazole contains two nitrogen atoms and one sulfur atom in its ring structure. It has four isomeric structures: 1,2,3-thiadiazole, 1,2,4-thiadiazole, 1,2,5-thiadiazole, and 1,3,5-thiadiazole (Fig. 1). Among all of them, 1,3,4-Thiadiazoles represent an important class of compounds and are widely used as pharmacophores due to their metabolic stability and ability to engage in hydrogen bonding[6-9]. 1,3,4-Thiadiazole is a conjugated, weakly basic, planar, and electron-deficient ring system (Fig. 1). Its high aromaticity, combined with the +I effect of sulfur, contributes to its weak basicity, while the electron-withdrawing nature of nitrogen atoms makes it electron-deficient. As a result, the carbon atoms at C-2 and C-5 are relatively inert to electrophilic substitution but more susceptible to nucleophilic attack. Substituents at these positions further activate the ring, enhancing nucleophilic reactivity. Although electrophilic attack

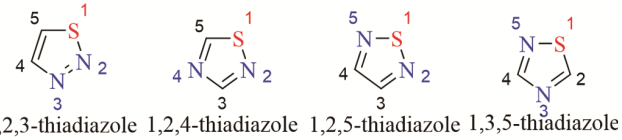

Fig. 1 — Isomeric structures of thiadiazole motif

on sulfur is uncommon, the ring nitrogen atoms can undergo such reactions depending on the substituents at C-2 or C-5. The ring structure is highly stable and resistant to aqueous acidic conditions but undergoes cleavage in strong basic environments. Various synthetic approaches have been developed for the preparation of 1,3,4-thiadiazoles and their derivatives[10-12]. A broad range of substituted 1,3,4-thiadiazoles has gained significant attention in drug discovery owing to their diverse pharmacological properties[13,14]. These azoles possess notable biological potential, as evidenced by numerous studies highlighting their anti-fungal[15], anti-microbial[16-19], anti-Alzheimers[20,21], anti-candidal[22], -anti-diabetic[23,24], anti-viral[25], and anti-cancer[26-31] activities.

Thiazoles have demonstrated remarkable efficacy against infectious diseases[32-34], showcasing their versatility in addressing various therapeutic challenges, including Chagas disease[35-37]. Chagas disease (CD), also known as American trypanosomiasis, was first discovered in 1909 by Brazilian physician Carlos Chagas[38]. It primarily affects impoverished communities with limited access to healthcare. Over 90% of global cases are concentrated in Argentina (1.5 million), Brazil (1.2 million), and Mexico (0.88 million). Bolivia has the highest prevalence, with 0.61 million cases. Significant case numbers are also reported in Colombia (0.44 million) and Venezuela (0.31 million), where the disease remains endemic[39]. This debilitating multisystem disorder is caused by the parasitic protozoan *Trypanosoma cruzi*[40]. Recent advancements have been made in the development of antitrypanosomal agents to combat trypanosomiasis caused by the *Trypanosoma* parasite. However, despite their significance, limited research has been conducted on the synthesis and medicinal potential of antitrypanosomal derivatives.

In this context, we designed and synthesized a novel library of thiadiazole–thiocoumarin hybrids (**A1–A10**) to explore their potential as multitarget agents. These molecules were assessed for *in vitro* activity against *T. cruzi*, *M. tuberculosis* H37Rv, *P. falciparum*, oxidative stress models (DPPH and ABTS radical scavenging), and microbial pathogens including *E. coli*, *S. aureus*, *C. albicans*, and others. To complement biological findings, a detailed structure–activity relationship (SAR) analysis was conducted to elucidate key physicochemical features underlying activity and selectivity. This study aims to identify thiadiazole–thiocoumarin hybrids that are not only potent but also cytocompatible, thereby offering leads for further development in neglected disease and antimicrobial pipelines.

Experimental Section

Analytical-grade chemicals obtained from commercial sources were used for compound preparation without further purification. Laboratory chemicals were supplied by Sigma-Aldrich and Fisher Scientific Ltd. Melting points were determined using the open-tube capillary method and were uncorrected. Thin-layer chromatography (TLC) with silica gel G and various eluant systems was employed to assess compound purity. Infrared spectra were recorded using Fourier transform infrared spectroscopy (FT-IR) with a Perkin Elmer RZX and an Agilent Resolution Pro FT-IR spectrometer, utilizing potassium bromide pellets, with frequencies expressed in cm^{-1}. ^{1}H NMR and ^{13}C NMR spectra were obtained on a Bruker Advance II 400 spectrometer (100 MHz FT-NMR) using tetramethyl silane as an internal standard in deuterochloroform ($CDCl_3$) and dimethyl sulfoxide (DMSO-d_6), with chemical shifts reported in δ ppm. Mass spectra were recorded using a WATERS Q-ToF Micro Mass spectrometer with electrospray ionization (ESI-MS). Column chromatography was performed on silica gel 60 (0.043–0.06 mm) from Merck. Elemental analysis was conducted on a Carlo Erba 1108 analyzer, with results deviating within ±0.04% of the calculated values.

Synthesis of 2-oxo-2*H*-thiochromen-4-yl-2-chloroacetate, **4** was carried out following the procedure described in the literature[41].

Synthesis of 5-substituted-1,3,4-thiadiazol-2-amine, 3a-j

To a stirred solution of thiosemicarbazide (0.5 mmol) in methanol (1 mL) and a solution of the substituted acid (0.5 mmol) in methanol (1 mL), a catalytic amount of $POCl_3$ was added. After being stirred at RT for 30 minutes, the reaction mixture was heated to reflux for 6-8 hrs. until the conversion was complete. The reaction progress was monitored by TLC (using Hexane: EtOAc, 3:7). After the completion of the reaction, the reaction mass was cooled at RT and poured over ice-cold water. The solid separated was filtered and treated with dil. NaOH. The resulting solid was washed with water and crystallized with methanol to make the pure product as an analytical sample.

General procedure for the synthesis of 2-oxo-2*H*-thiochromene-4-yl-(5-substituted-1,3,4-thiadiazol-2-yl) glycinate, A1-10

In a borosilicate flask, 0.01 mol of 5-substituted-1, 3, 4-thiadiazol-2-amine **3a-j**, 0.02 mol of anhydrous K_2CO_3, and 0.01 mol of 2-oxo-2*H*-thiochromen-4-yl-2-chloroacetate (4) were mixed in DMF and the mixture was refluxed for 6-8 hours. The reaction progress was monitored by TLC (Toluene: MeOH: EtOAc, 3:3:4). After the completion of the process, the resulting mixture was poured over crushed ice with constant stirring. Solids separated were filtered, dried, and recrystallized with DMF ethanol to get titled compounds **A1-10**.

5-(4-Aminophenyl)-1,3,4-thiadiazol-2-amine, IA2: IR (KBr): 3505, 3486 (NH_2), 3053 (C-H aromatic), 1640 (N=C), 1245 (C-N), 750 cm^{-1} (C-S); ^{1}H NMR (DMSO-d_6): δ 7.20 (s, 2H, -NH_2, thiadiazol), 6.58-7.76 (m, 4H, aromatic), 5.26 (s, 2H, -NH_2); ^{13}C NMR (100MHz, DMSO-d_6): δ 174 (C_2, N=C-N), 161.8 (C_5, N=C-S), 145.9 (C_{10}), 129.1 (C_8 & C_{12}), 123.2 (C_7), 115.5 (C_9 & C_{11}); ESI–MS: *m/z* Calcd 192.24. Found 193.05 $[M + H]^+$.

2-Oxo-2*H*-thiochromen-4-yl (5-(4-hydroxyphenyl)-1,3,4-thiadiazol-2-yl)glycinate, A1: IR (KBr): 3545 (OH), 3383 (NH), 3025 (C-H aromatic), 1738 (-COO), 1672 (C=O), 1642 (N=C), 1250 (C-N), 745 cm^{-1} (C-S); ^{1}H NMR (DMSO-d_6): δ 9.66 (s, 1H, OH), 7.02-7.80 (m, 8H, aromatic), 6.05 (s, 1H, -CH), 5.87 (s, 1H, -NH), 4.02 (s, 2H, -CH_2); ^{13}C NMR (100MHz, DMSO-d_6): δ 183.4 (C_{18}, C=O, α,β-unsaturated compound), 172.4 (C_7, N=C-N), 167.3 (C_1, -COO), 164.5 (C_{10}, N=C-S), 161.5 (C_{14}), 160.6 (C_{20}), 134.2 (C_{26}), 131.3 (C_{24}), 129.1 (C_{25}), 127.6 (C_{22}), 127.5 (C_{23}), 127.2 (C_{12} & C_{16}), 125 (C_{11}), 119.5 (C_{21}), 115.7 (C_{13} & C_{15}), 114.5 (C_{19}, CH), 48.2 (C_3, CH_2); ESI–MS: *m/z* Calcd 411.45. Found 412.04 $[M + H]^+$.

2-Oxo-2*H*-thiochromen-4-yl (5-(4-aminophenyl)-1, 3,4-thiadiazol-2-yl)glycinate, A2: IR (KBr): 3487 (NH_2), 3387 (NH), 3024 (C-H aromatic), 1742 (-COO), 1670 (C=O), 1632 (N=C), 1265 (C-N), 738 cm^{-1} (C-S); ^{1}H NMR (DMSO-d_6): δ 6.87-7.74 (m, 8H, aromatic), 6.07 (s, 1H, -CH), 5.95 (s, 1H, -NH), 5.24 (s, 2H, NH_2), 4.00 (s, 2H, -CH_2); ^{13}C NMR (100MHz, DMSO-d_6)δ (ppm): 183.5 (C_{18}, C=O, α,β-unsaturated compound), 172.6 (C_7, N=C-N), 167.1 (C_1, -COO), 164.7 (C_{10}, N=C-S), 160.5 (C_{20}), 156.6 (C_{14}), 134 (C_{26}), 131.1 (C_{24}), 129.6 (C_{25}), 127.4 (C_{22}), 127.6 (C_{23}), 127.3 (C_{12} & C_{16}), 125.3 (C_{11}), 119.2 (C_{21}), 114.6 (C_{19}, CH), 114.2 (C_{13} & C_{15}), 48.5 (C_3, CH_2); ESI–MS: *m/z* Calcd 410.47. Found 411.05 $[M + H]^+$.

2-Oxo-2*H*-thiochromene-4-yl-(5-(4-nitrophenyl)-1,3,4-thiadiazol-2-yl)glycinate, A3: IR (KBr): 3385 (NH), 3022 (C-H aromatic), 1735 (-COO), 1670 (C=O), 1640 (N=C), 1520, 1511 (-NO_2), 1265 (C-N), 743 cm^{-1} (C-S); ^{1}H NMR (DMSO-d_6): δ 7.11-8.32 (m, 8H, aromatic), 6.09 (s, 1H, -CH), 5.88 (s, 1H, -NH), 4.00 (s, 2H, -CH_2); ^{13}C NMR (100MHz, DMSO-d_6): δ 185.2 (C_{20}, C=O, α,β-unsaturated compound), 174 (C_7, N=C-N), 167 (C_1, -COO), 164 (C_{10}, N=C-S), 160.5 (C_{22}), 148 (C_{14}), 139.8 (C_{11}), 135.6 (C_{28}), 134 (C_{26}), 128.4 (C_{27}), 128 (C_{24}), 127.5 (C_{25}), 126.8 (C_{12} & C_{16}), 125.5 (C_{13} & C_{15}), 124 (C_{23}), 103 (C_{21}, CH), 44 (C_3, CH_2); ESI–MS: *m/z* Calcd 440.45. Found 441.03 $[M + H]^+$.

2-Oxo-2*H*-thiochromen-4-yl (5-(4-chlorophenyl)-1,3,4-thiadiazol-2-yl)glycinate, A4: IR (KBr): 3390 (NH), 3021 (C-H aromatic), 1748 (-COO), 1675 (C=O), 1630 (N=C), 1260 (C-N), 733 (C-S), 545 cm^{-1} (C-Cl); ^{1}H NMR (DMSO-d_6): δ 7.15-8.02 (m, 8H, aromatic), 6.06 (s, 1H, -CH), 5.94 (s, 1H, -NH), 4.01 (s, 2H, -CH_2); ^{13}C NMR (100MHz, DMSO-d_6): δ 183.3 (C_{18}, C=O, α,β-unsaturated compound), 172.4 (C_7, N=C-N), 167.3 (C_1, -COO), 164.6 (C_{10}, N=C-S), 160.4 (C_{20}), 136.6 (C_{14}), 134.2 (C_{26}), 133.8 (C_{11}), 131.3 (C_{24}), 129.1 (C_{25}), 129 (C_{13} & C_{15}), 127.6 (C_{22}), 127.5 (C_{23}), 127.3 (C_{12} & C_{16}), 119.2 (C_{21}), 114.6 (C_{19}, CH), 48.2 (C_3, CH_2); ESI–MS: *m/z* Calcd 429.89. Found 431 $[M + H]^+$.

2-Oxo-2*H*-thiochromene-4-yl-(5-(4-bromo phenyl)-1,3,4-thiadiazol-2-yl)glycinate, A5: IR (KBr): 3325 (NH), 3050 (C-H aromatic), 1724 (-COO), 1620 (C=O), 1240 (C-N), 760 (C-S), 551 cm^{-1} (C-Br); ^{1}H NMR (DMSO-d_6): δ 7.11-7.90 (m, 8H, aromatic), 6.00 (s, 1H, -CH), 5.96 (s, 1H, -NH), 4.02 (s, 2H, -CH_2); ^{13}C NMR (100MHz, DMSO-d_6): δ 185.4 (C_{18}, C=O, α,β-unsaturated compound), 174.1 (C_7, N=C-N), 167 (C_1, -COO), 164.2 (C_{10}, N=C-S), 160.3 (C_{20}), 134.1 (C_{26}), 133.7 (C_{11}), 132.2 (C_{13} & C_{15}), 131.4 (C_{24}), 129.5 (C_{25}), 129 (C_{12} & C_{16}), 127.8 (C_{22}), 127.4 (C_{23}), 125 (C_{14}), 119.5 (C_{21}), 114.4 (C_{19}, CH), 43.8 (C_3, CH_2) ESI–MS: *m/z* Calcd 474.35. Found 472.95 $[M+H]^+$.

2-Oxo-2*H*-thiochromen-4-yl(5-(2-amino-4-chlorophenyl)-1,3,4-thiadiazol-2-yl)glycinate, A6: IR (KBr): 3502 (NH_2), 3388 (NH), 3018 (C-H aromatic), 1740 (-COO), 1672 (C=O), 1634 (N=C), 1263 (C-N), 729 (C-S), 548 cm^{-1} (C-Cl); ^{1}H NMR (DMSO-d_6): δ 6.99-7.56 (m, 7H, aromatic), 6.02 (s, 1H, -CH), 5.97 (s, 1H, -NH), 5.79 (s, 2H, NH_2), 4.03 (s, 2H, -CH_2); ^{13}C NMR (100MHz, DMSO-d_6): δ 183.1 (C_{19}, C=O, α,β-unsaturated compound), 172.1 (C_7, N=C-N), 167.3 (C_1, -COO), 160.6 (C_{21}), 153 (C_{10}, N=C-S), 148.2 (C_{12}), 136.3 (C_{14}), 134.2 (C_{27}), 131.3 (C_{25}), 129 (C_{26}), 127.6 (C_{23}), 127.5 (C_{24}), 126.1 (C_{16}), 119.9 (C_{11}), 119.5 (C_{22}), 117.5 (C_{15}), 116.8 (C_{13}), 114.6 (C_{20}, CH), 48.6 (C_3, CH_2); ESI–MS: *m/z* Calcd 444.91. Found 446.01 $[M + H]^+$.

2-Oxo-2*H*-thiochromen-4-yl (5-(4-iodophenyl)-1,3,4-thiadiazol-2-yl)glycinate, A7: IR (KBr): 3386 (NH), 3017 (C-H aromatic), 1741 (-COO), 1673 (C=O), 1627 (N=C), 1259 (C-N), 738 (C-S), 550 cm^{-1} (C-I); ^{1}H NMR (DMSO-d_6): δ 7.15-7.95 (m, 8H, aromatic), 6.04 (s, 1H, -CH), 5.93 (s, 1H, -NH), 4.04 (s, 2H, -CH_2); ^{13}C NMR (100MHz, DMSO-d_6): δ 183.2 (C_{18}, C=O, α,β-unsaturated compound), 172.3 (C_7, N=C-N), 167.2 (C_1, -COO), 164.8 (C_{10}, N=C-S), 160.7 (C_{20}), 137.8 (C_{13} & C_{15}), 134.2 (C_{26}), 133.3 (C_{11}), 131.1 (C_{24}), 129.4 (C_{12} & C_{16}), 129.1 (C_{25}), 127.6 (C_{22}), 127.5 (C_{23}), 119.5 (C_{21}), 114.7 (C_{19}, CH), 93.1 (C_{14}), 48.1 (C_3, CH_2); ESI–MS: *m/z* Calcd 521.35. Found 521.94 $[M + H]^+$.

2-Oxo-2*H*-thiochromene-4-yl-(5-(pyridin-4-yl)-1,3,4-thiadiazol-2-yl)glycinate, A8: IR (KBr): 3350 (NH), 3020 (C-H aromatic), 1733 (-COO), 1672 (C=O), 1630 (N=C), 1262 (C-N), 740 cm^{-1} (C-S); ^{1}H NMR (DMSO-d_6): δ 7.11-8.80 (m, 8H, aromatic), 6.05 (s, 1H, -CH), 5.88 (s, 1H, -NH), 4.02 (s, 2H, -CH_2); ^{13}C NMR (100MHz, DMSO-d_6): δ 185.2 (C_{17}, C=O, α,β-unsaturated compound), 174.1 (C_7, N=C-N), 167 (C_1, -COO), 164 (C_{10}, N=C-S), 160.7 (C_{19}), 150 (C_{11} & C_{15}), 135.6 (C_{13}), 134 (C_{25}), 131.3 (C_{23}), 129.1 (C_{24}), 127.5 (C_{21}), 126.8 (C_{22}), 125.5 (C_{12} & C_{14}), 125 (C_{20}), 121 (C_{18}, CH), 44.0 (C_3, CH_2); ESI–MS: *m/z* Calcd 396.44. Found 397.04 $[M+H]^+$.

2-Oxo-2*H*-thiochromen-4-yl (5-(7-chloro-6-fluoro-4-oxo-1,4-dihydroquinolin-3-yl)-1,3,4-thiadiazol-2-yl)glycinate, A9: IR (KBr): 3500 (NH, aromatic), 3385 (NH, aliphatic), 3010 (C-H aromatic), 1748 (-COO), 1670 (C=O), 1624 (N=C), 1262 (C-N), 731 (C-S), 555 (C-F), 550 cm^{-1} (C-Cl); ^{1}H NMR (DMSO-d_6): δ 13.2 (s, 1H, NH, aromatic), 7.15-7.37 (m, 7H, aromatic), 6.00 (s, 1H, -CH), 5.96 (s, 1H, -NH), 4.08 (s, 2H, -CH_2); ^{13}C NMR (100MHz, DMSO-d_6): δ 183.4 (C_{24}, C=O, α,β-unsaturated compound), 174.6 (C_{14}, C=O, dihydroquinoline), 171.6 (C_7, N=C-N), 167.3 (C_1, -COO), 160.8 (C_{26}), 156.2 (C_{17}), 151.6 (C_{10}, N=C-S), 136.4 (C_{12}), 134.5 (C_{20}), 134.2 (C_{32}), 131.3 (C_{30}), 129.1 (C_{31}), 127.6 (C_{28}), 127.5 (C_{29}), 127.2 (C_{18}), 123.7 (C_{15}), 119.4 (C_{27}), 116.7 (C_{19}), 114.6 (C_{25}, CH), 108.7 (C_{13}), 108.6 (C_{16}), 48.8 (C_3, CH_2); ESI–MS: *m/z* Calcd 514.93. Found 515.99 $[M + H]^+$.

2-Oxo-2*H*-thiochromen-4-yl (5-(7-chloro-6-fluoro-8-methoxy-1-(1-methylcyclopropyl)-4-oxo-1,4-dihydroquinolin-3-yl)-1,3,4-thiadiazol-2-yl)glycinate, A10: IR (KBr): 3383 (NH), 3014 (C-H aromatic), 1744 (-COO), 1674 (C=O), 1640 (N=C), 1261 (C-N), 739 (C-S), 554 (C-F), 536 cm^{-1} (C-Cl); ^{1}H NMR (DMSO-d_6): δ 6.99-7.37 (m, 6H, aromatic), 6.06 (s, 1H, -CH), 5.91 (s, 1H, -NH), 4.00 (s, 2H, -CH_2), 3.83 (s, 3H, OCH_3), 1.35 (s, 3H, CH_3), 0.21 & 0.46 (m, 4H, cyclopropane); ^{13}C NMR (100MHz, DMSO-d_6): δ 183.8 (C_{30}, C=O, α,β-unsaturated compound), 173 (C_{14}, C=O, dihydroquinoline), 171.4 (C_7, N=C-N), 167.1 (C_1, -COO), 160.6 (C_{32}), 153.2 (C_{17}), 151.1 (C_{10}, N=C-S), 142.4 (C_{12}), 138.8 (C_{19}), 134 (C_{38}), 131.1 (C_{36}), 129.3 (C_{37}), 127.5 (C_{34}), 127.2 (C_{35}), 125.9 (C_{15}), 125.8 (C_{20}), 125.1 (C_{18}), 119.5 (C_{33}), 116.4 (C_{13}), 114.6 (C_{31}, CH), 104.4 (C_{16}), 60.6 (C_{27}), 48.6 (C_3, CH_2), 45.4 (C_{22}), 24.6 (C_{25}), 11.9 (C_{23} & C_{24}); ESI–MS: *m/z* Calcd 599.05. Found 600.05 $[M + H]^+$.

Result and Discussion

Chemistry

The synthesis of the thiadiazole–thiocoumarin hybrid derivatives **A1–A10** was accomplished through a concise and efficient pathway as outlined in Scheme 1. The synthetic strategy was initiated with the condensation of commercially available substituted salicylaldehydes and ethyl acetoacetate to afford intermediate coumarin derivatives *via* the Pechmann reaction. These intermediates were subsequently chlorinated to activate the coumarin core for nucleophilic substitution. Parallel to this, a set of 2-amino-1,3,4-thiadiazole derivatives were synthesized by the cyclization of thiosemicarbazide with various aromatic carboxylic acids under acidic conditions. The final step involved nucleophilic

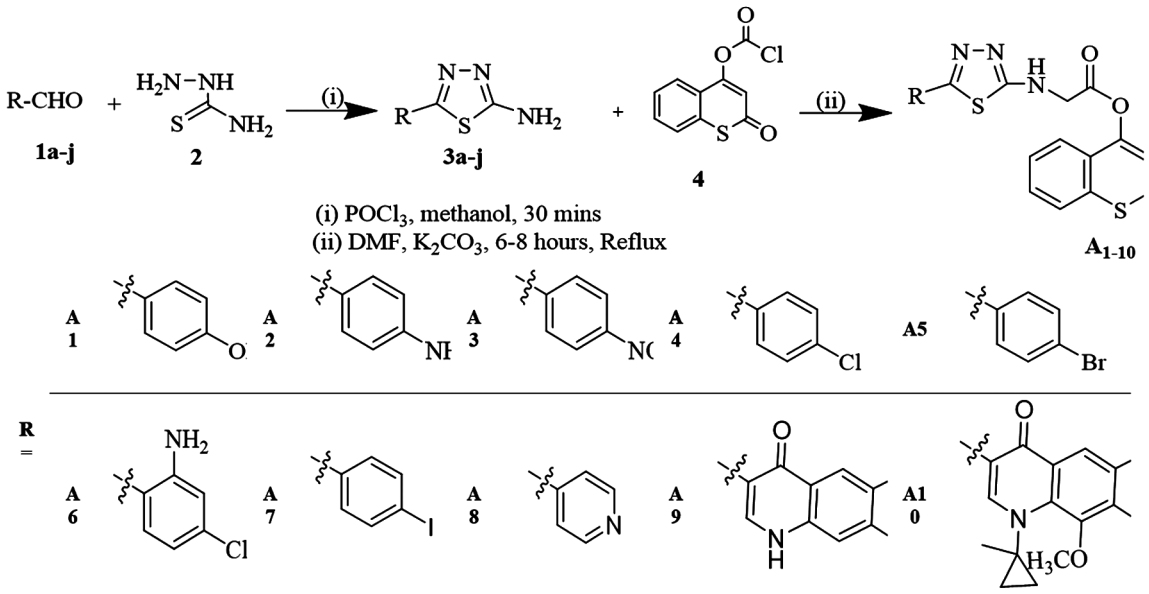

Scheme 1 — General Synthetic pathway for final compounds **A1-10**

substitution between the chlorinated coumarin derivatives and the thiadiazole amines, yielding the desired hybrids (**A1–A10**) in moderate to excellent yields (75–89%). The structures of the synthesized compounds were confirmed through spectroscopic techniques, including IR, ^{1}H and ^{13}C NMR, and mass spectrometry, with selected spectral data provided in the Supplementary Information. Characteristic peaks such as the C=N stretch (~1590–1615 cm^{-1}), aromatic proton resonances in the δ 7.2–8.5 ppm range, and thiadiazole-specific carbon signals (δ ~165 ppm) validated successful formation of the hybrid scaffolds. The detailed physical parameters of the synthesized compounds, including melting point, yield, and molecular formula, are summarized in Table 1. Overall, the synthetic route proved reproducible, and the incorporation of various electron-withdrawing and electron-donating substituents on the coumarin moiety enabled systematic evaluation of structure–activity relationships in subsequent biological assays.

Biological Evaluation

Cytotoxicity screening was performed against the J774A murine macrophage cell line to evaluate the host cell safety of the synthesized thiadiazole-thiocoumarin hybrids. The compounds demonstrated a broad range of cytotoxicity, with CC_{50} values varying from 116.8 µM to 847.6 µM (Table 2 and Fig. 2 and Fig. 3). Notably, **A9** (CC_{50} = 847.6 µM) and **A6** (697.8 µM) exhibited the highest cytocompatibility, whereas **A10** was the most cytotoxic among the series (CC_{50} = 116.8 µM). The selectivity index (SI), calculated as the ratio of CC_{50} to IC_{50}, indicated that **A9** (SI = 23.75 *vs* NINOA) and **A6** (SI = 19.84 *vs* INC-5) possess the highest therapeutic windows. These findings validate their promise as selective antiparasitic candidates. Structure–activity exploration revealed that, derivatives bearing halogenated aryl substituents, particularly with *para*-fluoro and *para*-chloro groups (**A9**, **A6**), showed increased selectivity and reduced host cell toxicity. Aromatic bulk appears to aid in selectivity without compromising safety when balanced with electron-withdrawing substituents.

The compounds were screened against *Trypanosoma cruzi* bloodstream trypomastigotes for strains such as NINOA and INC-5 (Table 3 and Fig. 4 and Fig. 5). Several derivatives demonstrated substantial lytic effects at 12.5 µg/mL, with **A9** (LC_{50} = 35.69 µM) and **A2** (LC_{50} = 50.91 µM) outperforming the reference drugs Benznidazole and Nifurtimox under similar conditions. Evaluation of substituent effects suggested that, high trypanocidal activity was associated with fluoro-chloro-diaryl substitution (**A9**) and trifluoromethylphenyl groups (**A2**). These features may enhance lipophilic interactions with the parasite membrane or inhibit parasite-specific redox enzymes. In contrast, unsubstituted or linear alkyl derivatives (**A1**, **A10**) were markedly less effective.

Primary screening against *Mycobacterium tuberculosis* H37Rv strain (Table 4 and Fig. 6)

Table 1 — Physical data of compounds **A1–A10**

Compd	R	Mol. Wt.	Yield (%)	m.p. (°C)	Mol. Formula
A1	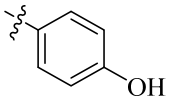	411.450	80	205-209	$C_{13}H_{13}N_3O_4S_2$
A2	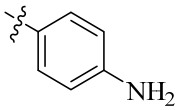	410.466	75	220-224	$C_{19}H_{14}N_4O_4S_2$
A3	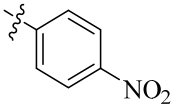	440.448	82	255-259	$C_{19}H_{12}N_4O_5S_2$
A4	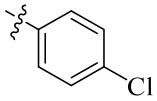	429.893	78	262-266	$C_{19}H_{12}N_3O_3S_2Cl$
A5	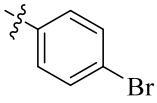	474.347	85	271-274	$C_{19}H_{12}N_3O_3S_2Br$
A6	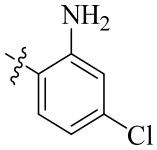	444.908	88	245-248	$C_{19}H_{13}N_4O_3S_2Cl$
A7	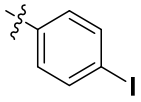	521.347	84	230-233	$C_{19}H_{12}N_3O_3S_2I$
A8	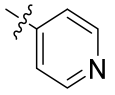	396.439	89	223-227	$C_{18}H_{12}N_4O_3S_2$
A9	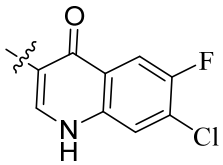	514.930	82	238-242	$C_{22}H_{12}N_4O_4S_2ClF$
A10	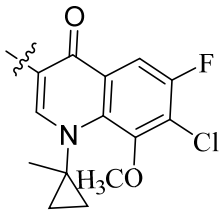	599.048	82	249-253	$C_{27}H_{20}N_4O_5S_2ClF$

Table 2 — Cytotoxic activity on murine macrophage cell line J774A

Compd	CC_{50} (μM)	Selectivity index	
		NINOA	INC-5
A1	558.9	> 3.34	> 6.11
A2	133.9	> 2.39	> 10.53
A3	635	11.66	6.03
A4	139.5	> 1.64	> 4.2

(*Contd.*)

Table 2 — Cytotoxic activity on murine macrophage cell line J774A (*Contd.*)

Compd	CC_{50} (μM)	Selectivity index	
		NINOA	INC-5
A6	697.8	10.28	19.84
A7	240	4.75	4.96
A8	605.3	> 4.64	> 3.43
A9	847.6	23.75	5.92
A10	116.8	> 1.59	> 0.99

Half maximal cytotoxic concentration (CC_{50}, μM) represented as the mean ±standard deviation (SD), three biological replicates; concentration that produces the cytotoxicity of 50% J774 cells.

Selectivity Index (SI): CC_{50} (μM) /IC_{50} (μM)

Table 3 — Percent Lysis at 12.5 μg/mL *in vitro* analysis on blood trypomastigotes

Compd	Cepa NINOA	Cepa INC-5	Cepa NINOA	Cepa INC-5
	Lysis at 12.5 μg/mL (%)		LC_{50} (μM)	
A1	6.02 ± 1.81	9.60 ± 1.75	167.11 ± 4.05	91.48 ± 4.35
A2	20.48 ± 3.13	10.86 ± 2.44	50.91 ± 4.24	79.78 ± 3.19
A3	15.66 ± 1.04	31.57 ± 1.91	54.46 ± 3.00	105.25 ± 6.05
A4	4.22 ± 1.81	26.26 ± 1.58	85.25 ± 2.74	33.26 ± 2.66
A5	5.42 ± 1.04	2.27 ± 2.00	80.67 ± 3.84	13.32 ± 2.91
A6	7.83 ± 1.81	37.12 ± 1.52	67.85 ± 1.91	35.17 ± 4.76
A7	21.69 ± 2.09	10.35 ± 0.44	50.54 ± 3.95	48.37 ± 3.48
A8	7.23 ± 2.09	19.70 ± 2.27	130.51 ± 3.74	176.72 ± 4.73
A9	9.64 ± 4.78	21.46 ± 1.16	35.69 ± 4.30	143.09 ± 19.25
A10	4.22 ± 1.81	51.26 ± 2.31	73.51 ± 2.69	117.35 ± 2.85
Benznidazol	32.20 ± 5.95	30.3 ± 5.45	177.79± 9.52	277.57 ± 11.33
Nifurtimox	28.57 ± 4.5	25.1 ± 3.57	199.09 ± 10.46	287.92 ± 8.97

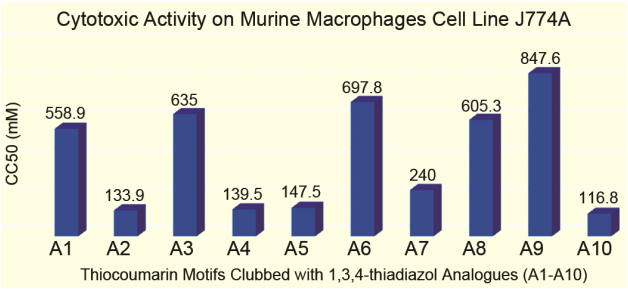

Fig. 2 — Cytotoxic activity as CC_{50} (μM) on murine macrophages cell line J774A

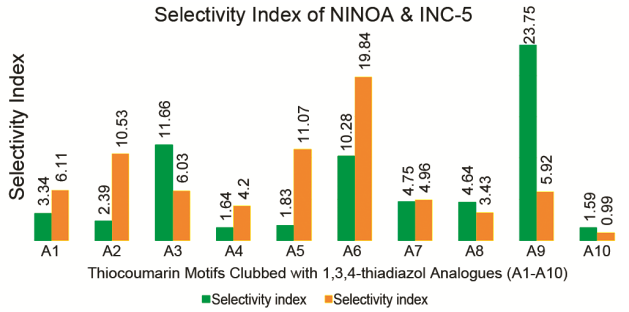

Fig. 3 — Selectivity index of NINOA and INC-5 on thiocoumarin motifs clubbed with 1,3,4-thiadiazol analogues (**A1–A10**)

revealed moderate activity across the series, with **A9** (MIC = 62.5 μg/mL) and **A8** (200 μg/mL) as the top performers. While none matched the potency of isoniazid (0.2 μg/mL), these compounds provide a promising structural basis for optimization. Systematic structure–activity relationship (SAR) analysis demonstrated, the presence of halogens on the coumarin ring (**A4–A9**) correlates with enhanced antimycobacterial potency, possibly *via* increased lipophilicity and better penetration into the mycobacterial cell wall. Iodinated compound **A7** was less active, suggesting that excessive steric bulk may limit permeability.

The compounds were screened against *Plasmodium falciparum* for chloroquine-sensitive strain (Table 5 and Fig. 7). The most active molecules were **A6** (IC_{50} = 0.58 μg/mL), **A9** (0.98 μg/mL), and **A4** (1.05 μg/mL). Evaluation of substituent effects suggested that optimal anti-plasmodial activity was observed with electron-deficient aryl groups (**A6**,

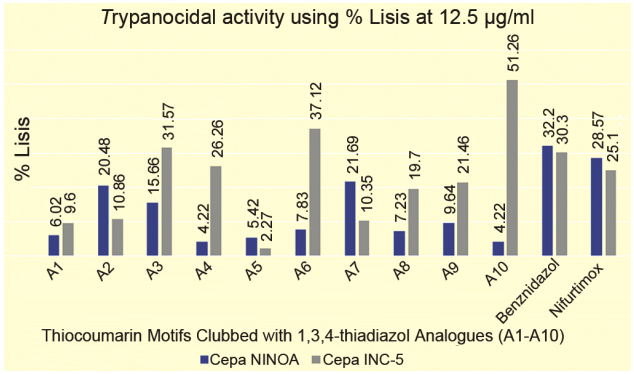

Fig. 4 — I*n vitro* trypanocidal activity using % lisis at 12.5 µg/mL for thiocoumarin motifs clubbed with 1,3,4-thiadiazol analogues (**A1–A10**)

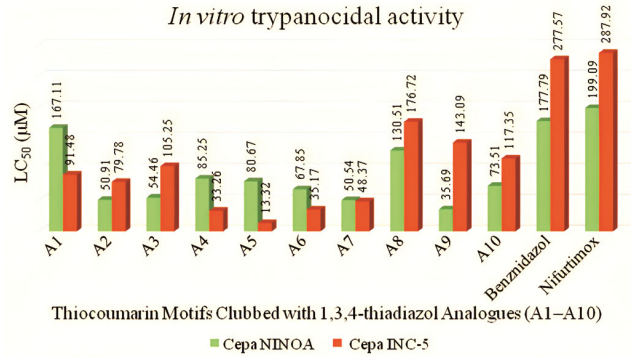

Fig. 5 — *In vitro* trypanocidal activity using LC_{50} (µM) for thiocoumarin motifs clubbed with 1,3,4-thiadiazol analogues (**A1–A10**)

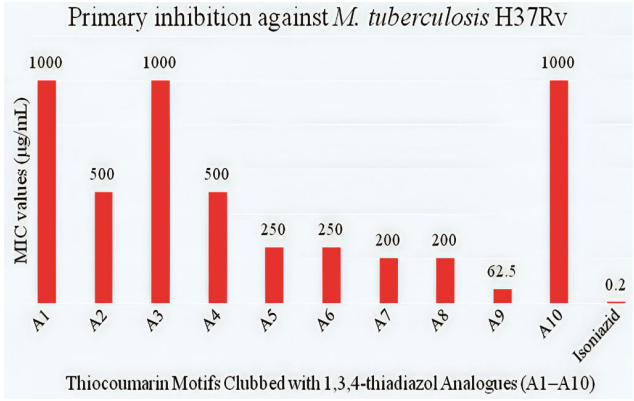

Fig. 6 — Primary inhibition against *M. tuberculosis H37Rv* for thiocoumarin motifs clubbed with 1,3,4-thiadiazol analogues (**A1–A10**)

A4), consistent with proposed heme-targeting mechanisms. The chloro- and fluoro-containing aryl substituents may improve π-π stacking interactions with heme moieties, disrupting parasite metabolism.

DPPH and ABTS assays were used to evaluate radical scavenging potential (Table 6 and Fig. 8). **A8**

Table 4 — Primary inhibition against *M. tuberculosis H37Rv* for thiocoumarin motifs clubbed with 1,3,4-thiadiazol analogues (**A1–A10**)

Compd	MIC values (µg/mL) of *M. tuberculosis H37Rv*
A1	1000
A2	500
A3	1000
A4	500
A5	250
A6	250
A7	200
A8	200
A9	62.5
A10	1000
Isoniazid	0.20

Table 5 — Antimalarial activity against *P. falciparum* for thiocoumarin motifs clubbed with 1,3,4-thiadiazol analogues (**A1–A10**)

Compd	Mean IC_{50} values (µg/mL) of *P. falciparum*
A1	2.16
A2	1.60
A3	1.45
A4	1.05
A5	1.09
A6	0.58
A7	1.32
A8	1.47
A9	0.98
A10	1.80
Chloroquine	0.20
Quinine	0.268

(DPPH IC_{50} = 33.92 µg/mL) and **A2** (35.33 µg/mL) exhibited strong antioxidant activity, while **A6** and **A7** showed the best ABTS scavenging. Antioxidant capacity was enhanced by electron-donating substituents or conjugated systems, such as in **A8** (dimethoxy aryl) and **A2** (fluorophenyl). Halogenated derivatives (**A5**, **A10**) showed weaker activity, likely due to limited hydrogen atom transfer potential.

Against bacterial and fungal strains (Table 7 and Fig. 9), compounds **A2**, **A4**, **A5**, and **A10** displayed notable activity, with MIC values between 25–100 µg/mL against *E. coli*, *S. aureus*, and *C. albicans*. **A10** demonstrated the broadest spectrum, despite higher cytotoxicity. Insights from SAR investigations indicated antibacterial efficacy correlated with moderate lipophilicity and electron-withdrawing aryl substituents, enabling membrane interaction. However, excessive bulk or poor

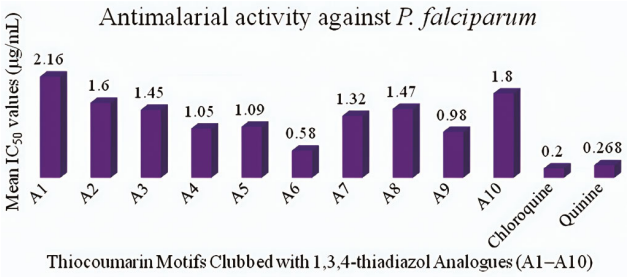

Fig. 7 — Antimalarial activity against *P. falciparum* for thiocoumarin motifs clubbed with 1,3,4-thiadiazol analogues (**A1–A10**)

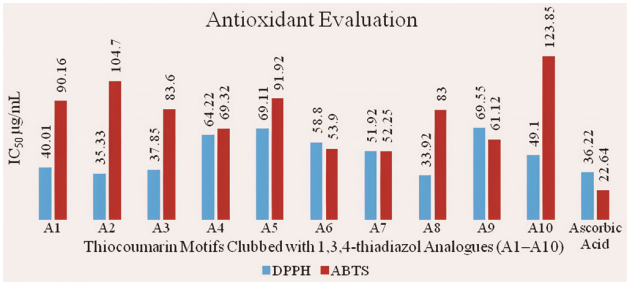

Fig. 8 — DPPH and ABTS radical scavenging activity for thiocoumarin motifs clubbed with 1,3,4-thiadiazol analogues (**A1–A10**)

Table 6 — Screening results of DPPH and ABTS radical scavenging activity for thiocoumarin motifs clubbed with 1,3,4-thiadiazol analogues (**A1–A10**)

Compd	DPPH	ABTS
	IC_{50} µg/mL ± SD	
A1	40.01 ± 0.192	90.16 ± 1.011
A2	35.33 ± 0.472	104.70 ± 0.754
A3	37.85 ± 0.247	83.60 ± 0.555
A4	64.22 ± 0.885	69.32 ± 0.823
A5	69.11 ± 0.856	91.92 ± 1.010
A6	58.80 ± 1.065	53.90 ± 0.757
A7	51.92 ± 1.090	52.25 ± 0.119
A8	33.92 ± 0.300	83.00 ± 0.723
A9	69.55 ± 0.335	61.12 ± 2.220
A10	49.10 ± 0.141	123.85 ± 1.051
Ascorbic Acid	36.22 ± 0.469	22.64 ± 0.260

Table 7 — Antimicrobial activity for thiocoumarin motifs clubbed with 1,3,4-thiadiazol analogues (**A1–A10**)

Compd	Minimal Bactericidal Concentration (µg/mL)				Minimal Fungicidal Concentration (µg/mL)		
	E.coli	*P.aeruginosa*	*S.Aureus*	*S.pyogenus*	*C.albicans*	*A.niger*	*A.clavatus*
	MTCC	MTCC	MTCC	MTCC	MTCC	MTCC	MTCC
	443	1688	96	442	227	228	1323
A1	250	125	250	500	500	1000	1000
A2	62.5	50	100	62.5	500	250	500
A3	100	250	125	100	>1000	500	>1000
A4	125	25	50	250	100	250	500
A5	100	62.5	100	100	250	500	>1000
A6	100	500	125	250	500	>1000	500
A7	100	125	250	500	>1000	>1000	>1000
A8	50	100	250	250	250	100	500
A9	62.5	250	500	250	500	500	>1000
A10	25	50	250	500	100	500	>1000
Gentamycin	0.05	1	0.25	0.5	–	–	–
Ampicillin	100	–	250	100	–	–	–
Chloramphenicol	50	50	50	50	–	–	–
Ciprofloxacin	25	25	50	50	–	–	–
Norfloxacin	10	10	10	10	–	–	–
Griseofulvin	–	–	–	–	500	100	100
Nystatin	–	–	–	–	100	100	100

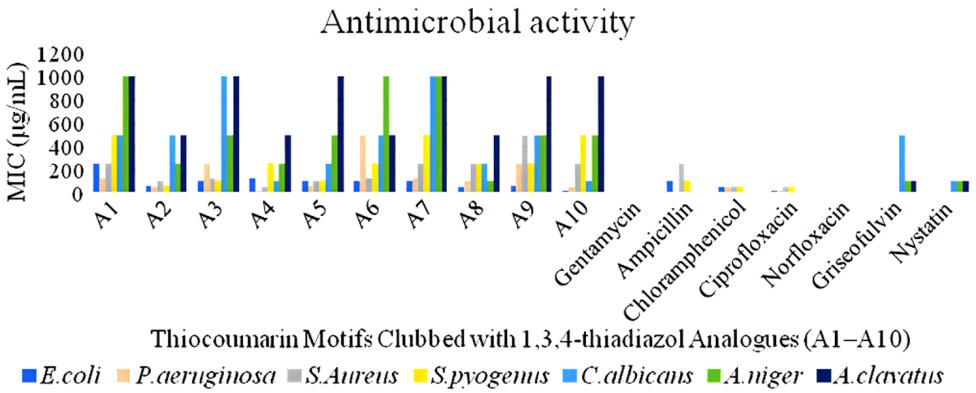

Fig. 9 — Antimicrobial activity for thiocoumarin motifs clubbed with 1,3,4-thiadiazol analogues (**A1–A10**)

Table 8 — SAR summary table

Substitution (R) Type	Key Compound (s)	Trypanocidal	Anti-TB	Antimalarial	Antioxidant	Antimicrobial	Cytotoxicity	SAR Summary
Fluoro-Chloro-Diaryl	A9	Excellent	Good	Good	Weak	Broad	Low	Ideal multitarget balance
Chloroaryl	A6	Moderate	Moderate	Best	ABTS	Weak	Safe	Strong antimalarial & safety
Trifluoromethylphenyl	A2	Good	Weak	Moderate	DPPH	Moderate	Moderate	Redox active, parasite-selective
Bromophenyl/ Iodophenyl	A5, A7	Weak	Moderate	Moderate	Weak	Moderate	Moderate	Bulky halogens reduce versatility
Dimethoxyaryl	A8	Weak	Moderate	Weak	Best	Weak	Safe	Selective antioxidant scaffold
Alkyl/ Unsubstituted	A1, A10	Poor	Weak	Moderate	Weak	Moderate	High (**A10**)	Limited bioactivity, high risk

solubility may reduce antifungal potency, as seen with **A7** and **A10**.

The structure–activity relationship across all biological assays highlights the impact of electronic, steric, and lipophilic tuning at the aryl substituent (Table 8). **A9** emerged as a true multitarget candidate, with favorable potency, selectivity, and cytocompatibility. **A6** demonstrated high efficacy in antimalarial and cytotoxic assays, ideal for further tuning. Compounds with bulky iodine or simple alkyl groups underperformed, indicating a need for electronic optimization. These insights provide a rational framework for future modifications, emphasizing halogenated diphenyl systems and conjugated electron-deficient moieties for broad-spectrum infectious disease therapy.

Conclusion

In this study, a novel series of thiadiazole–thiocoumarin hybrid derivatives (**A1–A10**) were successfully synthesized and comprehensively evaluated for their multitarget biological potential. The molecules demonstrated broad-spectrum activities against key pathogens including *Trypanosoma cruzi*, *Mycobacterium tuberculosis*, *Plasmodium falciparum*, bacterial and fungal strains, alongside significant antioxidant effects. The most promising compound, **A9**, exhibited potent trypanocidal activity (LC_{50} = 35.69 µM), antitubercular inhibition (MIC = 62.5 µg/mL), and noteworthy antimalarial efficacy (IC_{50} = 0.98 µg/mL), while maintaining low cytotoxicity (CC_{50} = 847.6 µM), resulting in one of the highest selectivity indices within the series. Additionally, compounds

A6, **A2**, and **A8** showed target-biased activity profiles, supporting their use in selective infectious disease treatment paradigms. The structure–activity relationship (SAR) analysis highlighted that electron-withdrawing halogenated aryl groups and moderate lipophilicity are essential for antiparasitic and antimicrobial activity, whereas electron-rich or fused aromatic systems favor antioxidant action and cyto-compatibility. These findings underscore the versatility of the thiadiazole–thiocoumarin scaffold as a platform for multitarget drug discovery. Collectively, this study lays the groundwork for the development of next-generation multitarget therapeutics based on thiadiazole–thiocoumarin hybrids for the treatment of neglected tropical diseases, tuberculosis, and antimicrobial-resistant infections.

Supplementary Information

Supplementary information is available in the website https://nopr.niscpr.res.in/handle/123456789/58776.

Acknowledgment

Miss Ankita S. Gamit appreciates the Ministry of Tribal Affairs, New Delhi, for granting the National Fellowship for Higher Education of ST Students (Award Number: 202122-NFST-GUJ-01273). Tejal Humal extends gratitude to the Gujarat State Education Department for supporting this research through the SHODH - Scheme of Developing High-Quality Research fellowship (Award Number: KCG/SHODH/2022-23/20210174134).

Conflict of Interest

The authors declared no conflict of interest.

References

1 Mukhrish Y E, Al-Humaidi J Y, Chagaleti B K, Albedair L A, Gomha S M, Saravanan V, Kathiravan M & Oubella A, *J Mol Struc*, 1322 (2025) 140385.
2 Mostefai M, Benmohammed A, Benhalima N, Dege N, Rahmani R, Kourat O, Guerroudj A R, Chouaih A, Djafri A, *J Mol Struc*, 1319 (2025) 139308.
3 Zaki Y H, Gomha S M, Farag B, Zaki M E & Hussein A M, *Results Chem*, 13 (2025) 101977.
4 Silva A L, Lima A C, Gonçalves J M, Morais, V M, Silva M D R D, *J Chem Thermo*, 202 (2025) 107423.
5 Dawood K M, Farghaly T A, *Expert Opinion Therap Pat*, 27 (2017) 477.
6 Laamari Y, Muhammed M T, Irfan A, Oubella A, Alossaimi M A, Geesi M H, Riadi Y, Taha M L, Morjani H & Auhmani A, *J Mol Struc*, 1319 (2025) 139368.
7 Serag M I, Tawfik S S, Eisa H M & Badr S M, *Drug Dev Res*, 86 (2025) e70035.
8 Kaya B, Çevik U A, Behçet M, Karayel A, Daoud N E-H, Bostancı H E & Kaplancıklı Z A, *J Mol Struc*, 1321 (2025) 140134.
9 An J-S, Hu S-H, Chen H-J, Fei Q & Wu W-N, *Phosphorous Sulfur Silicon Relat Elem*, 200 (2025) 372.
10 Ahmad S, Alam M Z, Salma U, Mohasin M, Rahaman P F, Parveen H & Khan S A, A *J Mol Struc*, 1312 (2024) 138438.
11 Abdulnabi N M & Tomi I H R, *J Mol Struc*, 1338 (2025) 142328.
12 Özkınalı S, Çavuş M, Tosun T, Şener N, Gür M & Şener İ, *J Mol Struc*, 1325 (2025) 140901.
13 Kumar D, Aggarwal N, Kumar V, Chopra H, Marwaha R K & Sharma R, *Fut Med Chem*, 16 (2024) 563.
14 Du W-R, Wang Y-X, Zhou X-W, Lan Y, Wei B-B, Guo X-Y, Wang X-K & Ma Z-Y, *Med Chem Res*, 34 (2025) 910.
15 Ibrahim A G, Elgammal W E, Hashem A H, Mohamed A E, Awad M A & Hassan S M, *Poly Bull*, 2024 (81) 1303.
16 Wu N, Yang Y, Tian G, An L, Liu S, Yan T, Yi M & Bao X, *J Agri Food Chem*, 71 (2023) 19277.
17 Serban G, Stanasel O, Serban E & Bota S, *Drug Design Devel Ther*, 12 (2018) 1545.
18 Ali A A, Soliman M A, Aouad M R, Messali M & Rezki N, *Org Prep Proc Int*, 51 (2019) 270.
19 Basir N F A, Nor Za'im S I, Ghafarikhaligh M, Johan M R & Khaligh N G, *J Sulf Chem*, 46 (2025) 656.
20 Hatami M, Basri Z, Sakhvidi B K & Mortazavi M, *Int Immunopharm*, 118 (2023) 110027.
21 Sujatha M, Jalihal P, Katagi M S, Bidye D P, Dixit S R & Nandeshwarappa B, *Russian J Bioorg Chem*, 51 (2025) 912.
22 Ouf S A, Gomha S M, Farag B, Zaki M E, Ewies M M, Sharawy I A, Khalil F O, Mahmoud H K, *Res Chem*, 7 (2024) 101406.
23 Taha M, Khan A A, Rahim F, Hayat S, Imran S, Iqbal N, Uddin N, Khan K M, Farooq R K & Nawaz M, *J Mol Struc*, 1282 (2023) 135173.
24 Al-Nasser F, Taha M, Rahim F, Adalat B, Chigurupati S, Nawaz M, Ajmal A, Wadood A, Uddin N & Khan K M, *J Mol Struc*, 1322 (2025) 140394.
25 Lohith T, Gayathri B, Feizi-Dehnayebi M, Kumar S, Divya K, Sridhar M, Mahendra M & Ziarani G M, *J Mol Struc*, 1330 (2025) 141356.
26 Santhosh C, Chinnam S, Kottam N, Amreen S, Ananthnag G S, Madhu G, Gadde S, Fernandes V T & Arnipalli H, *Res Chem*, 13 (2024) 101939.
27 Gür M, Yerlikaya S, Şener N, Özkınalı S, Baloglu M C, Gökçe H, Altunoglu Y C, Demir S & Şener İ, *J Mol Struc*, 1219 (2020) 128570.
28 Obakachi V A, Kushwaha B, Kushwaha N D, Mokoena S, Ganai A M, Pathan T K, Van Zyl W E, Karpoormath R, *J Sulf Chem*, 42 (2021) 670.
29 Reddy P S, Sekhar T, Thriveni P, Kumar G M, Rao A T, Raish M, Giridhar T & Srinivasulu G, *Res Chem*, 14 (2025) 102093.
30 Yurttaş L, Evren A E, AlChaib H, Temel H E & Akalin Çiftçi G, *J Biomole Struc Dyn*, *43* (2025) 3814.
31 Sharma S, Shamanth S, Siddiqua H, Goyary L, Sagar K S, Kumari S, Sathees D, Radha G, Choudhary B,

Raghavan S C & Mantelingu K, *Eur J Med Chem Rep*, 13 (2025) 100247.
32 Mohammed M H & Jabbar S A-S, *Mate Today*: *Proc*, 61 (2022) 710.
33 Sonawane K, Said R & Hatvate N, *S-Heterocycles*: *Retrospect*, *Prospects*, *and Biological Applications*, (Royal Society of Chemistry, UK), 2024, p. 163-223.
34 Fatima S, Saeed A, Babar A, Ejaz S A, Ahmed A, Shabir G & Zaman H, *J Mol Struc*, *1331* (2025) 141567.
35 De S, Aamna B, Sahu R, Parida S, Behera S K & Dan A K, *Eur J Med Chem*, 240 (2022) 114576.
36 Kumar A, Kaushal A, Verma P K, Gupta M K, Chandra G, Kumar U, Yadav A K & Kumar D, *Eur J Med Chem*, 280 (2024) 116896.
37 Akhtar J, Khan A A, Ali Z, Haider R & Yar M S, *Eur J Med Chem*, 125 (2017) 143.
38 Com B M B B, Putting Chagas disease on the global health agenda. *BMC medicine*, 21 (2023) 188.
39 Mills R M, *Ame J Med*, 133 (2020) 1262.
40 Martín-Escolano J, Marín C, Rosales M J, Tsaousis A D, Medina-Carmona E & Martín-Escolano R, *ACS Inf Dis*, 8 (2022) 1107.
41 Tiwari M R & Patel N B, *Curr Micro Chem*, 8 (2021) 33.